

# Investigating the Effect of Boundary Excitation on the Orientation Behavior of Non-Spherical Grains Using the Discrete Element Method (DEM)

By

Saeed Naamnh

B.Sc., Jordan University of Science and Technology, Jordan, 2014

M.Sc., Hungarian University of Agriculture and Life Sciences, Hungary, 2019

A Project Report Submitted in Partial Fulfillment of the Requirements for the Degree of

MASTER OF ENGINEERING

in the Department of Mechanical Engineering

© Saeed Naamnh, 2024  
University of Victoria

All rights reserved. This project report may not be reproduced in whole or in part, by photocopy or other means, without the permission of the author.

# Investigating the Effect of Boundary Excitation on the Orientation Behavior of Non-Spherical Grains Using the Discrete Element Method (DEM)

By

Saeed Naamnh

B.Sc., Jordan University of Science and Technology, Jordan, 2014

M.Sc., Hungarian University of Agriculture and Life Sciences, Hungary, 2019

## Supervisory Committee

Dr. Ben Nadler, Supervisor  
Department of Mechanical Engineering

Dr. Rustom Bhiladvala, Department Member  
Department of Mechanical Engineering

## Abstract

Non-spherical grains have been progressively receiving attention from the research communities and industry due to their natural occurrence and relevance in engineered applications. These grains display complex behaviors that are associated with different applications such as agriculture and the pharmaceutical industries. However, they also pose significant challenges such as jamming when passing through constricted pathways. Most existing studies on granular materials have focused on spherical grains, emphasizing grain size rather than shape and orientation, particularly in relation to grain-boundary interactions. Studies have shown that the mechanical properties of non-spherical grains are significantly influenced by their alignment. This has been demonstrated through various simulations and experimental investigations.

This study investigates the orientation behavior of non-spherical grains in response to oscillating boundaries using the Discrete Element Method (DEM). The results reveal that boundary excitation plays a pivotal role in influencing grain alignment, offering new insights into how excitation drives grain alignment. It is observed that as the boundary excitation increases the degree of alignment decreases, indicating a strong dependence of orientation behavior on excitation parameters such as frequency. Additionally, the variations in grain shape is found to significantly influence the alignment.

**Keywords:** Discrete Element Method (DEM), oscillating boundaries, grain orientation, non-spherical grains.

# Contents

|  |            |
|--|------------|
| <b>Abstract</b>                        | <b>iii</b> |
| <b>Acknowledgments</b>                 | <b>vii</b> |
| <b>1 Introduction</b>                  | <b>1</b>   |
| 1.1 Granular mechanics                 | 1          |
| 1.2 Literature Review                  | 2          |
| 1.3 Orientation representation         | 4          |
| 1.4 Objectives                         | 5          |
| 1.5 Report Outline                     | 6          |
| <b>2 Discrete Element Method (DEM)</b> | <b>7</b>   |
| <b>3 Results and Discussion</b>        | <b>11</b>  |
| 3.1 The effect of grains agitation     | 13         |
| 3.2 The effect of aspect ratio         | 16         |
| <b>4 Conclusion</b>                    | <b>18</b>  |
| <b>References</b>                      | <b>19</b>  |

## List of Figures

|    |  |    |
|----|--|----|
| 1  | Examples of non-spherical granular materials.  | 1  |
| 2  | Dimensions and orientation for non-spherical grain.  | 4  |
| 3  | Representation of the simulation domain containing non-spherical grains.   | 9  |
| 4  | Random distribution of the generated grains before excitation.   | 10 |
| 5  | The Cubic container with non-spherical grains when the excitation is applied from different sources (red walls).   | 12 |
| 6  | Top view. Alignment of non-spherical grains after agitation from different sources, (a) case 1, (b) case 2.  | 13 |
| 7  | Comparison of the order parameter, $\zeta$ , over dimensionless time, $\hat{t} = tf$ , where, $t$ , is time in seconds, for two aspect ratios ( $AR$ ) and three frequency ( $f$ ) values. | 14 |
| 8  | Variation of the orientation angle, $\alpha$ , over, $\hat{t}$ , showing its dependence on the excitation direction.   | 15 |
| 9  | Evolution of the order parameter, over, $\hat{t} = tf$ , during excitation.  | 16 |
| 10 | Top view. Non-spherical grains alignment after agitation (a) $AR = 4$ . (b) $AR = 2$ .   | 17 |

## List of Tables

- |   |  |    |
|---|--|----|
| 1 | The simulation parameters and particle properties. | 11 |
|---|--|----|

## **Acknowledgments**

I would like immensely to express my heartfelt gratitude to my supervisor for their invaluable guidance throughout this research. I am also deeply thankful to my colleagues and family for their encouragement and support.

# 1 Introduction

## 1.1 Granular mechanics

Granular materials are large collections of discrete solid particles with sizes large enough that Brownian motion is irrelevant [1]. Common examples of granular materials are sand and soil, these materials are also commonly encountered in many fields such as food products like seeds, rice, corn and sugar, as well as chemical and pharmaceutical products like pills and powders. Granular particles vary greatly in shape and size, ranging from micron sized powders to few meters sized blocks in rock avalanches. Figure 1 shows examples of granular materials.



Figure 1: Examples of non-spherical granular materials.

Granular materials can behave like a solid, or like a fluid. Such behaviors depend on particle size, shape, and the excitations applied. Most of granular flows, involve non-spherical grains. Currently, the studies in this field consider only the size, often neglecting the shape of the grains and their effect on

orientation during flow. Hence, investigating how grain shape influences their orientation during flow becomes vital.

## 1.2 Literature Review

Spherical grains exhibit a simpler mechanical response compared to non-spherical grains because their symmetrical shape ensures that grain orientation has no impact on their interactions. In contrast, non-spherical grains like spherocylinders have a well defined orientation that plays a significant role in how grains interact through contact [2].

The orientation of non-spherical grains is strongly influenced by their shape. The shape also greatly impacts the degree of grain alignment, with more elongated grains showing a greater degree of alignment. As reported by several studies, such as [3], which explored the influence of particle shape on sheared dense granular media, it was observed that for elongated particles, the orientation is strongly dependent on their shape.

Reddy [4] proposed an order parameter to measure the degree of orientational alignment of the grains. This parameter ranges from 0 to 1, with 0 indicating isotropic particle orientation and 1 indicating all particles are perfectly aligned. The study also observed that the alignment increases with increasing grain aspect ratio. The aspect ratio of the grain can be defined as the ratio of its length ( $l$ ) to its width or diameter ( $d$ ):

$$AR = \frac{l}{d} \tag{1}$$

A notable observation was reported by [4], highlighting the tendency of non-spherical particles to align themselves when subjected to shear. This orientation is characterized by the average orientation angle, representing the angle between the mean orientation of the particles and the flow's streamlines. Notably, this angle is not zero and decreases with an increase in the length-to-width aspect ratio of the particles. According to the observation by Nagy [5] who noted that the number of collisions for non-spherical grains is higher compared to spherical grains. Supporting this, Azema [6] reported that interactions between non-spherical grains can occur over an area of grain surface, unlike spherical grains, which interact only at a single contact point. The flow behavior of the granular system emerges from the interactions and movements of individual grains. The movement of each grain is influenced by a mix of external forces, such as gravity and contact forces arising from interactions with adjacent grains. With this concept as a foundation, the discrete element method (DEM) was developed by Cundall & Strack in 1979 [7]. DEM uses parameters such as solid volume fraction (the ratio of the volume of solid particles to the total volume), velocity, size, and shape to predict the motion, interactions, and the behavior of granular systems. However due to its high resolution down to the individual grains, a significant increase in computational demands as the number of grains in the system grows. As observed by many DEM practitioners like Cleary [8], when the particle count exceeds 10 million, simulations using DEM are often avoided due to the limitations of current computing capabilities.

In this study, grains are created as clumped spheres to represent non-spherical

shape for DEM simulation. This method models complex grain shapes by overlapping and bonding spheres, enabling the representation of any particle shape. Additionally, contact detection and force calculations remain efficient by leveraging well-established interactions for spherical particles. As highlighted by [9], the clumped spheres approach is one of the most widely used technique in the DEM community.

### 1.3 Orientation representation

The orientation of non-spherical grains, can be distinctly and clearly defined by the direction along their axis of symmetry  $\pm \mathbf{k}$  as shown in Figure 2.

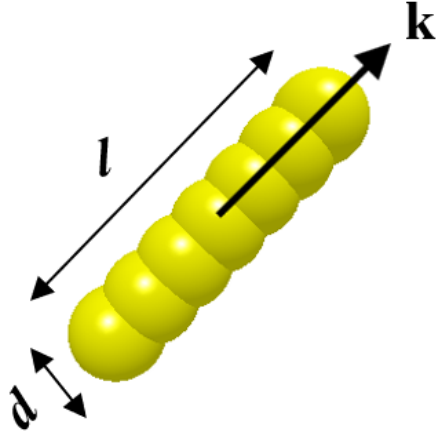


Figure 2: Dimensions and orientation for non-spherical grain.

The orientation is defined by the dyad  $(\mathbf{k}_i \otimes \mathbf{k}_i)$ . For assembly of grains (N), the averaged orientational tensor takes the form as defined by [10]:

$$\mathbf{A} = \frac{1}{N} \sum_{i=1}^N (\mathbf{k}_i \otimes \mathbf{k}_i) \quad (2)$$

where N is the number of grains and  $(\mathbf{k}_i \otimes \mathbf{k}_i)$  is the orientation of the  $i$ -th grain. It follows from equation (5) that the orientational tensor is positive

semi-definite and symmetric with  $tr\mathbf{A} = 1$ . The orientational tensor  $\mathbf{A}$  has three eigenvalues and three eigenvectors, which define the principal axes of orientation. The eigenvector associated with the largest eigenvalue  $a_1$  represents the primary direction of alignment where  $1 \geq a_1 \geq a_2 \geq a_3 \geq 0$ . In this study, the degree of grain alignment is represented as an ordering measure, as defined by [10]:

$$\zeta = \sqrt{\frac{1}{2} ((a_1 - a_2)^2 + (a_2 - a_3)^2 + (a_3 - a_1)^2)} \quad (3)$$

Where  $\zeta$  is the order parameter. The limiting case of  $\zeta = 0$  corresponds to random distribution, while  $\zeta = 1$  is when all grains are aligned.

## 1.4 Objectives

This study investigates the alignment of non-spherical grains within a closed cubic container, where two opposing walls oscillate back and forth move in opposite direction. The analysis is conducted using the Discrete Element Method (DEM) as a numerical tool. The main objectives of this study include:

- Investigating the influence of the non-spherical grain shapes on alignment behavior under the effect of the oscillating boundaries.
- Investigating the order parameter and analyzing its revolution with time.
- Investigating the role of agitation variation on alignment behavior.

## 1.5 Report Outline

This report is organized into four chapters, each of which contributes to the overall understanding of the subject. A brief overview of the following chapters is provided below:

- **Chapter 2:** Discrete Element Method (DEM)

This chapter presents the implementation of the discrete element method, detailing the essential parameters and providing a description of the boundary conditions used in the simulation.

- **Chapter 3 :** Simulation, Results, and Discussion

This chapter presents the results obtained from the DEM simulation and provides an analysis of the findings. It also explores the role of parameters such as aspect ratio and frequency on grains orientation.

- **Chapter 4:** Conclusions

The final chapter presents a summary of the key findings and conclusions derived from this study.

## 2 Discrete Element Method (DEM)

In the Discrete Element Method (DEM), each particle, denoted as particle  $i$  obeys Newton's second law of motion for translation and rotation, the translational motion is determined by calculating the net force acting on the particle, while the rotational motion is governed by the net torque resulting from collisions and body force. This approach allows for the individual tracking of each particle's motion by explicitly solving for its trajectory over time. The process involves calculating the forces and torques acting on each particle, which are then used to determine the particle's acceleration and orientation at each time step. This particle-level tracking provides a detailed representation of granular flow dynamics.

### 1. Translational Motion

The translational motion of particle  $i$  is described by Newton's second law as:

$$m_i \frac{d^2 \mathbf{x}_i}{dt^2} = \mathbf{F}_i^{\text{ext}} + \sum_{j=1}^{N_i} \mathbf{F}_{ij}^{\text{contact}} \quad (4)$$

Where:

- $m_i$  is the mass of the particle  $i$ .
- $\mathbf{x}_i$  is the position vector of particle  $i$ .
- $\mathbf{F}_i^{\text{ext}}$  represents the external forces (such as gravity) acting on particle  $i$ .
- $\mathbf{F}_{ij}^{\text{contact}}$  is the contact force between particle  $i$  and neighboring particles  $j$ .

- $N_i$  is the number of neighboring particles  $j$  interacting with particle  $i$ .

The contact forces  $\mathbf{F}_{ij}^{\text{contact}}$  are decomposed into normal and tangential components. In the current study, grains are assumed to be frictionless. Therefore, only the normal contact force is considered and no tangential contact force is present. Considering frictionless grains simplifies the analysis by reducing the computational complexity and focusing on the effect of grain shape.

$$\mathbf{F}_{ij}^{\text{contact}} = \mathbf{F}_{ij}^{\text{normal}} \quad (5)$$

Where:

- $\mathbf{F}_{ij}^{\text{normal}}$  is the normal force component that prevents particle overlap.

## 2. Rotational Motion

The rotational motion of particle  $i$  follows Newton's second law for rotation:

$$\mathbf{I}_i \frac{d\boldsymbol{\omega}_i}{dt} = \mathbf{T}_i \quad (6)$$

Where:

- $\mathbf{I}_i$  is the moment of inertia of the particle  $i$ , which depends on its shape and mass distribution.
- $\boldsymbol{\omega}_i$  is the angular velocity of the particle  $i$ .
- $\mathbf{T}_i$  represents the total torque acting on the particle  $i$  due to contact forces and body force.

In this study, the Hertz-Mindlin contact law is utilized to implement a DEM simulation. This law, where the normal force component is based on the Hertz model [11], was applied using EDEM<sup>®</sup> software. EDEM<sup>®</sup> [12] is chosen as its user-friendly interface and advanced built-in 3D visualization tools, which facilitate the analysis of particle motion and contact forces. The normal force has damping component to account for energy dissipation during collision, where the damping coefficient is related to the coefficient of restitution as described in [13]. The coefficient of restitution is the ratio of post-collision to pre-collision relative velocity.

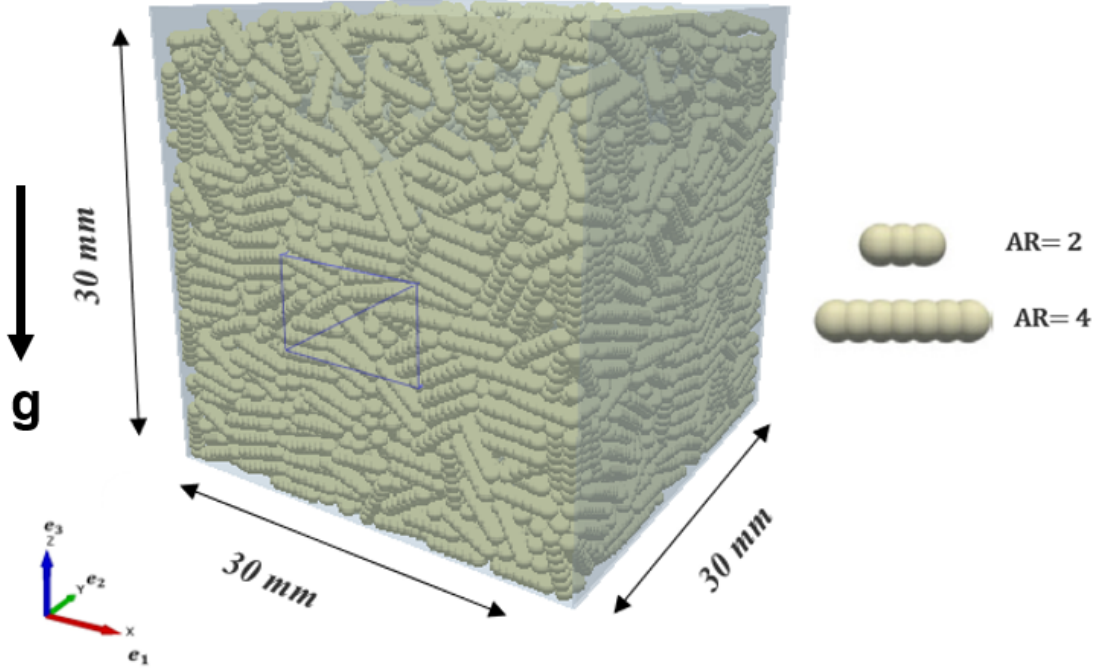


Figure 3: Representation of the simulation domain containing non-spherical grains.

The DEM simulation, carried out in a 3D closed cubic container, is shown in Figure 3. The grains are generated to fill this domain randomly as shown in Figure 4. The grains are selected as spherocylinders with diameters of 1

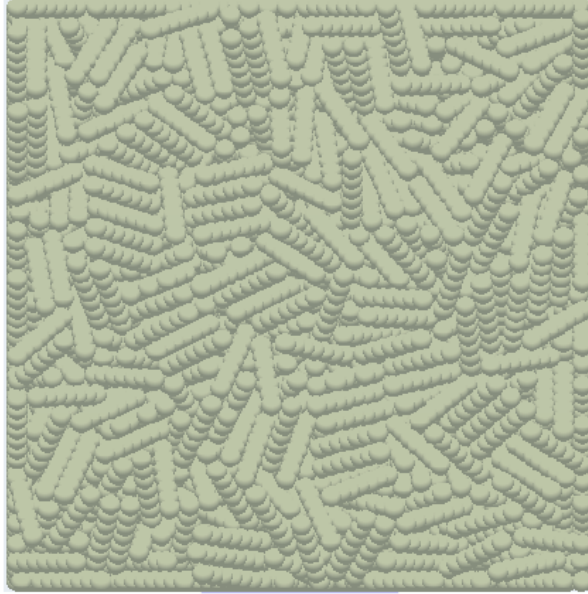


Figure 4: Random distribution of the generated grains before excitation.

mm, and lengths of 2.0 mm or 4.0 mm, resulting in aspect ratios of 2.0 and 4.0, these dimensions are chosen to minimize high computational time while ensuring meaningful results. Increasing the aspect ratio requires more spheres to form the elongated shape, leading to a higher number of contact points and increased computational time. The amplitude of the walls are set to be small ( $\pm 0.5\text{mm}$ ), with excitation applied at frequencies of 100, 500, and 1000 Hz. The solid volume fraction of the grains is set to ( $\nu = 0.67$ ), ensuring a dense medium and strong collisions. It is important to mention that for spherical grains solid volume fraction must remain below ( $\nu = 0.64$ ) where exceeding this value the ability of the spherical grains to flow drop significantly as observed by [14]. However, this limitation does not apply for spherocylinders. Collision properties are defined with a coefficient of restitution of ( $e = 0.95$ ) for grains, this value indicates highly elastic collisions. Frictional interactions are simplified with coefficients of static and rolling friction set to zero. The

parameters used in the simulation are defined in Table 1.

Table 1: The simulation parameters and particle properties.

| <b>Material Properties</b>      | <b>Particle</b> |
|---------------------------------|-----------------|
| Particle Diameter (mm)          | 1               |
| Particle Length (mm)            | 2.0, 4.0        |
| Aspect Ratio                    | 2.0, 4.0        |
| Solid Volume Fraction ( $\nu$ ) | 0.67            |
| Number of Particles ( $N$ )     | 5000            |
| <b>Collision Properties</b>     |                 |
| Coefficient of Restitution      | 0.95            |
| Coefficient of Static Friction  | 0.0             |
| Coefficient of Rolling Friction | 0.0             |

### 3 Results and Discussion

When the excitations are applied, the walls, as shown in Figure 5, oscillate opposite to each other, while the container remains stationary. The grains interact with oscillating walls, experience translational and rotational motion due to collisions. In case 1, as shown in Figure 5.a, the oscillation of the walls

causes the grains to agitate, leading them to rotate and align normal to the oscillating walls, as illustrated in Figure 6.a. Once the grains have aligned, the excitation source is changed by altering the wall oscillation, as shown in Figure 5.b. In case 2, as shown in Figure 5.b, the wall oscillation induces agitation, causing the grains to reorient and align in a different direction. This behavior is further demonstrated in Figure 6.b. This change in excitation source leads to a transition in grain's orientation as they gradually realign over the time with the new direction of oscillation as shown in Figure 6.b. To demonstrate the boundary effect due to the agitation, virtual control volume has been created. This control volume is placed in the center (highlighted in orange), as shown in Figure 6.

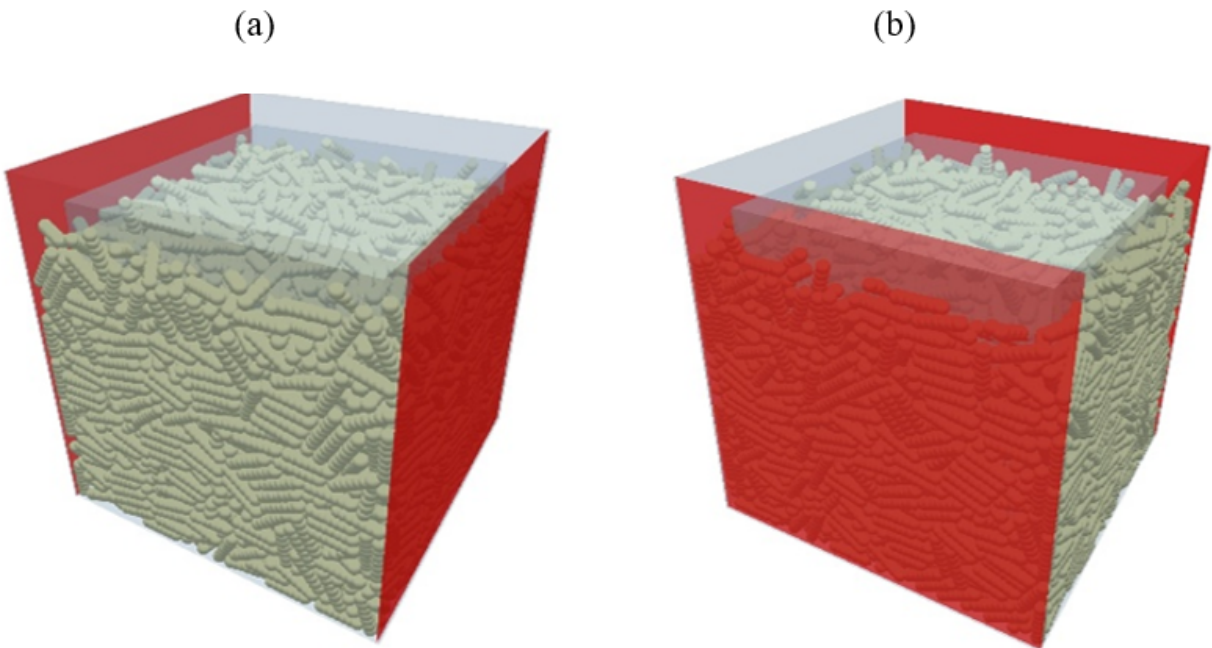


Figure 5: The Cubic container with non-spherical grains when the excitation is applied from different sources (red walls).

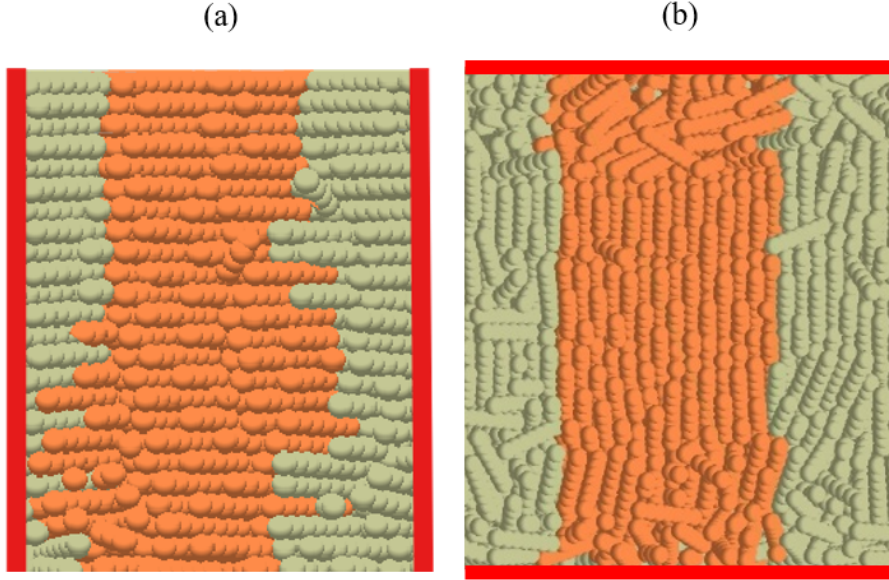


Figure 6: Top view. Alignment of non-spherical grains after agitation from different sources, (a) case 1, (b) case 2.

### 3.1 The effect of grains agitation

Applying excitation agitates the grains, increasing the randomness of their motion. This agitation sufficiently influences the alignment of non-spherical grains through collisions and interactions. Generally, at higher excitation frequencies, the increased agitation causes the grains to move more randomly, thereby reducing their ability to achieve alignment. Conversely, at lower excitation frequencies, the reduced agitation allows the grains to align as they rotate or adjust their orientation due to interactions.

The results indicate that for grains with an aspect ratio ( $AR = 4$ ), the alignment occurs, but the alignment degree varies with the frequency values. As the value of frequency increases, the alignment decreases. As shown in Figure 7, the alignment occurs at (100 Hz) with order parameter approaching 0.9, indicating a high degree of alignment. After achieving alignment at (100 Hz),

the frequency is increased to 500 Hz and 1000 Hz to observe the behavior of the grains at higher frequencies. At these frequencies, the alignment reduces significantly due to the increased agitation of the grains.

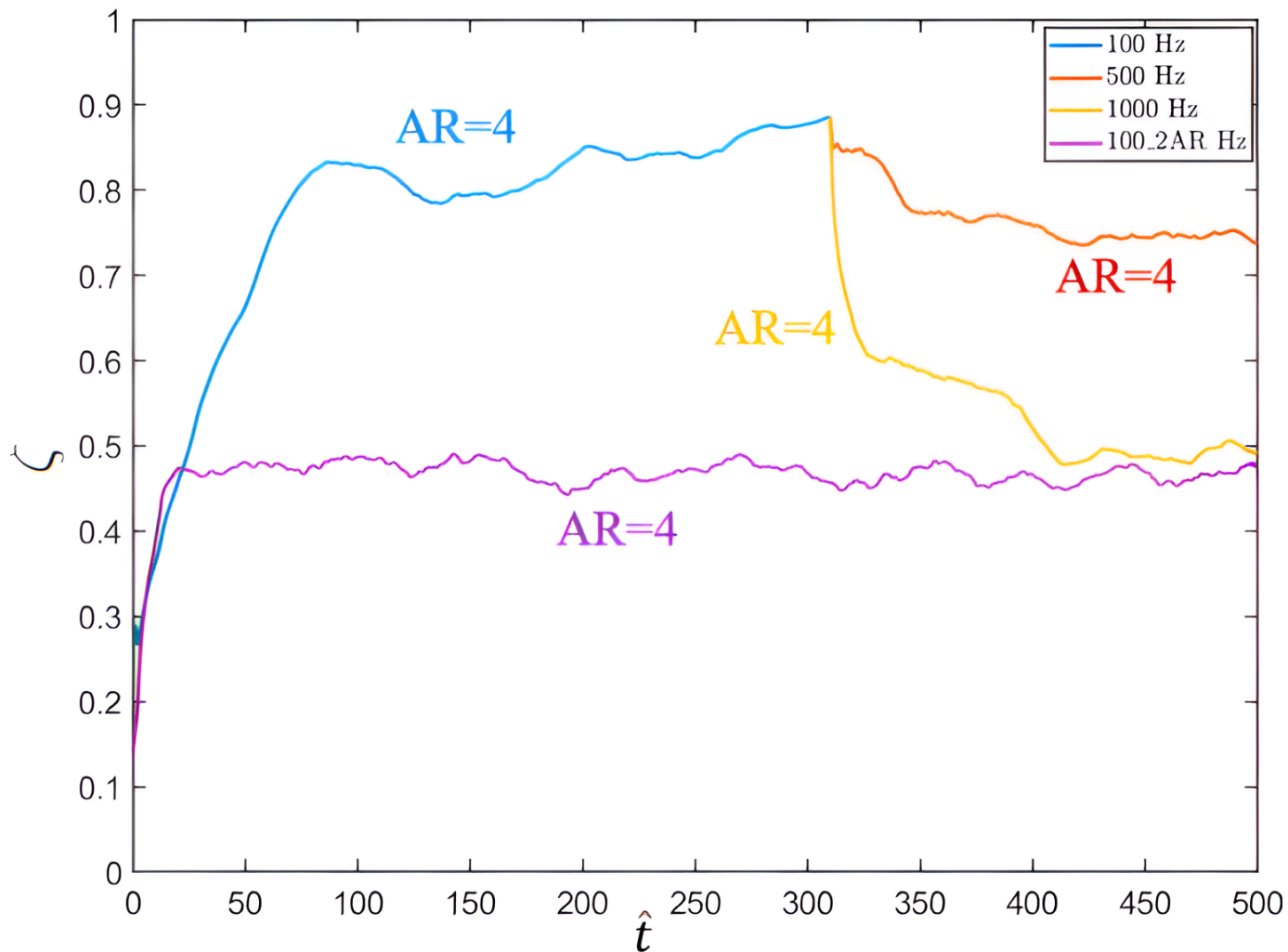


Figure 7: Comparison of the order parameter,  $\zeta$ , over dimensionless time,  $\hat{t} = tf$ , where,  $t$ , is time in seconds, for two aspect ratios ( $AR$ ) and three frequency ( $f$ ) values.

The orientation angle ( $\alpha$ ), presented in Figure 8, is analyzed to illustrate its behavior to changes in agitation source. When the excitation source is switched to case 2, a significant change is observed in the behavior of ( $\alpha$ ). The angle increases rapidly as the grains reorient, eventually reaching a steady-state that aligns with the new excitation direction.

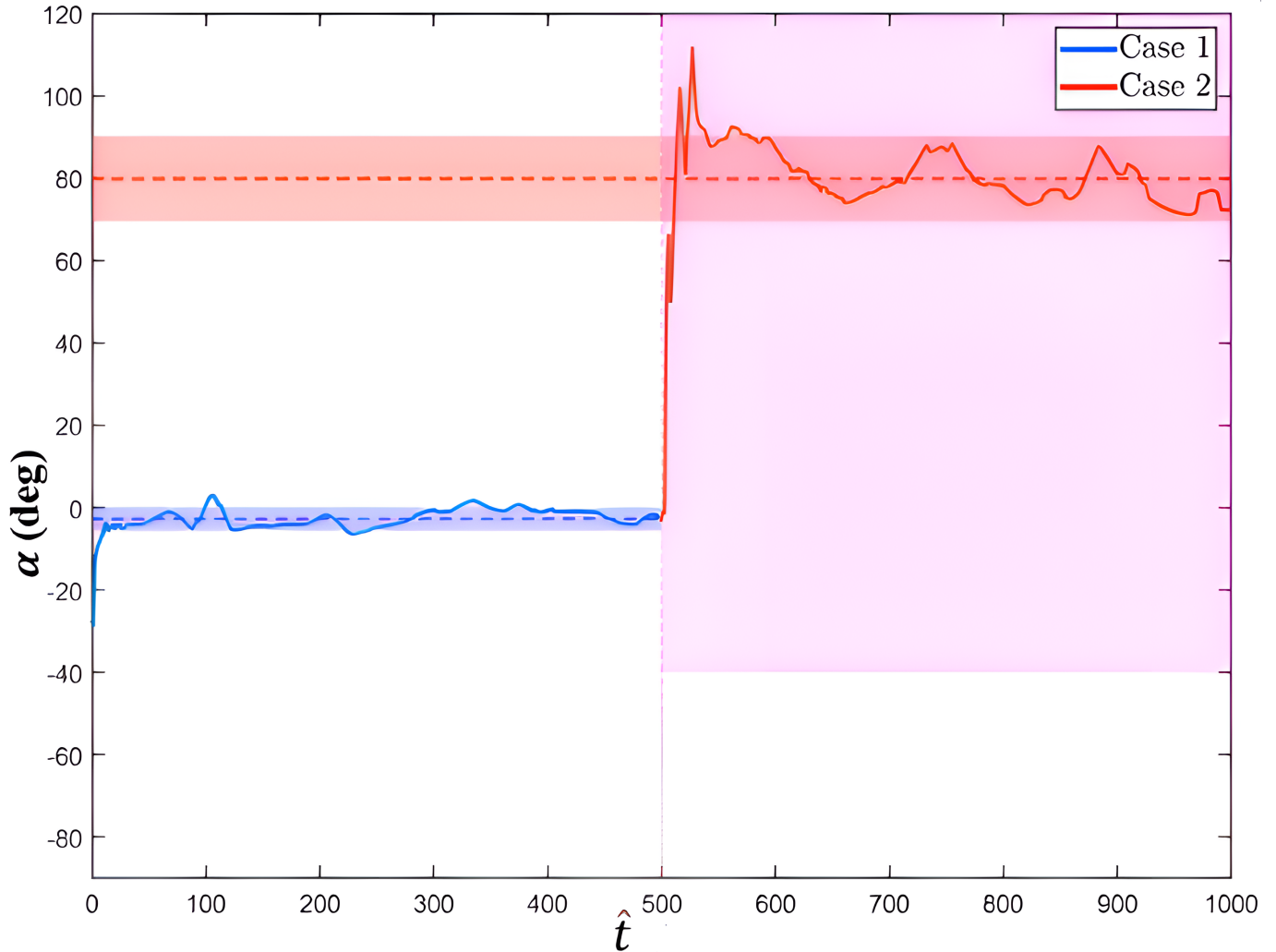


Figure 8: Variation of the orientation angle,  $\alpha$ , over,  $\hat{t}$ , showing its dependence on the excitation direction.

The analysis highlights how the non-spherical grains adjust their orientation when the agitation source switched, as evidenced by the evolution of  $(\alpha)$  and  $(\zeta)$  as shown in Figure 8 and 9 respectively. The steady-state of  $(\alpha)$  near  $80^\circ$  and the subsequent increase in  $(\zeta)$  demonstrate the grains' ability to adapt to the new agitation source while maintaining a high degree of alignment.

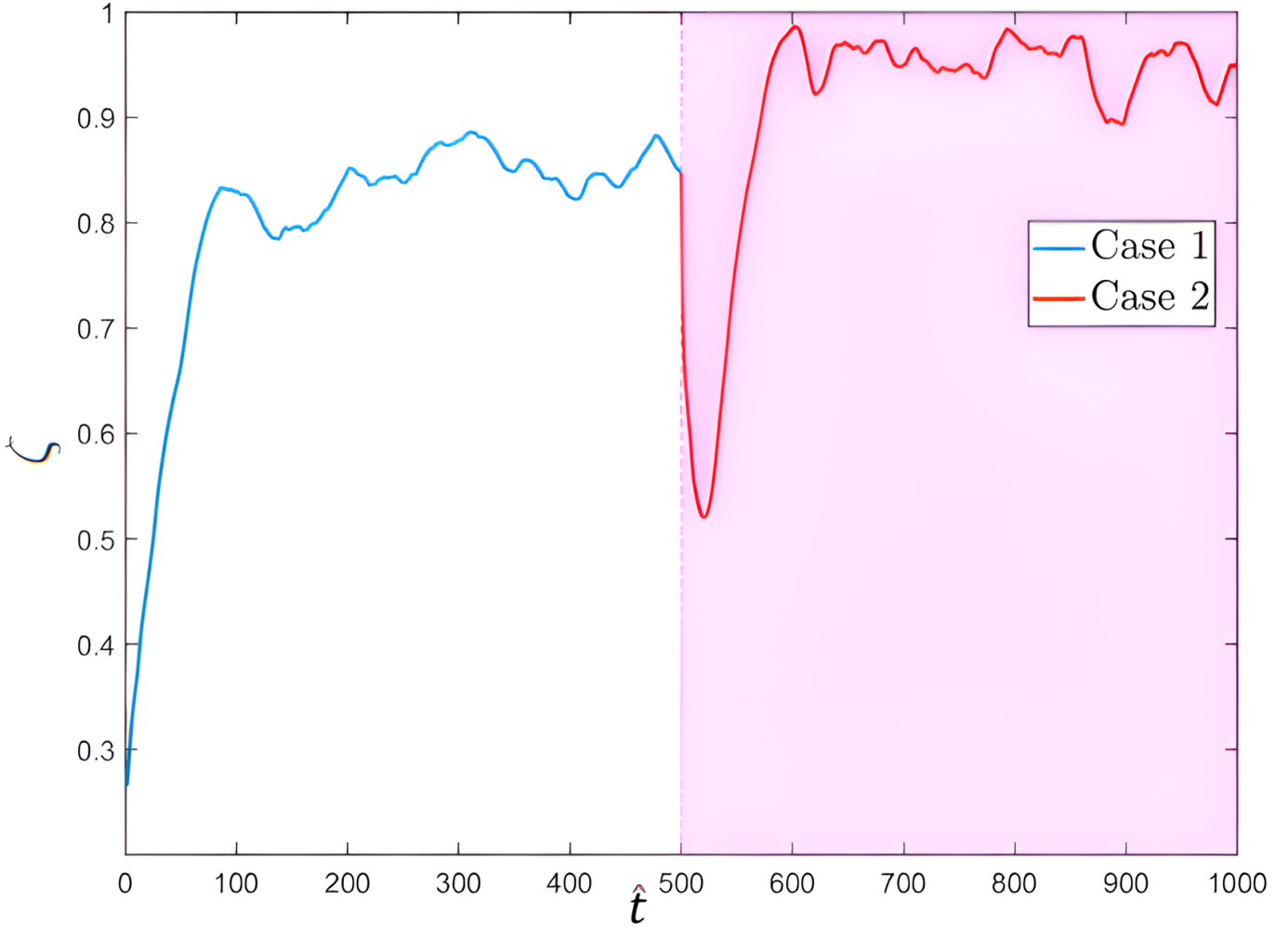


Figure 9: Evolution of the order parameter, over,  $\hat{t} = tf$ , during excitation.

### 3.2 The effect of aspect ratio

The aspect ratio ( $AR$ ) of grains plays a crucial role in their tendency to achieve alignment. Figure 7 shows grains with higher aspect ratios ( $AR$ ) exhibit a greater tendency to align.

As the aspect ratio increases, the order parameter, ( $\zeta$ ), increases, reflecting a strong tendency toward a highly ordered, aligned state. This behavior underscores the sensitivity of grain alignment to aspect ratio. Conversely, grains with lower aspect ratios show more random alignments, resulting in reduced

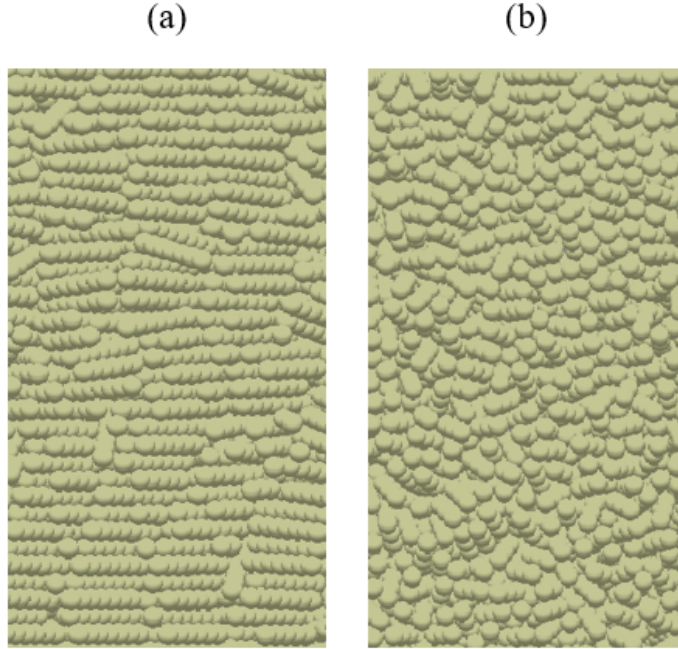


Figure 10: Top view. Non-spherical grains alignment after agitation (a)  $AR = 4$ . (b)  $AR = 2$ .

( $\zeta$ ) values. Figure 7 demonstrates that non-spherical grains with ( $AR = 4$ ) align under lower agitation (e.g., at 100 Hz), achieving a high degree of alignment. In contrast, grains with ( $AR = 2$ ) display less degree of alignment at the same frequency, indicating a reduced ability to align under same excitation values. This disparity arises from the lower aspect ratios of the grains, which reduce their sensitivity to agitation. Figure 10. illustrates the alignment of the non-spherical grains after excitation with two different aspect ratios ( $AR$ ). The grains with ( $AR = 4$ ) exhibit high alignment, as shown in Figure 10.a, while the grains with ( $AR = 2$ ) show less alignment compared to ( $AR = 4$ ), as shown in Figure 10.b.

## 4 Conclusion

In this study, the effects of boundary excitation and aspect ratio on the alignment of non-spherical grains were investigated to better understand the relationship between the agitation and grain shape. The findings revealed that the agitation significantly influences the grain alignment. High excitation promotes the randomization due to increased grains agitation, whereas low excitation facilitates alignment by reducing the agitation allowing grains to adjust their orientation. The results demonstrated that the alignment varies with excitation frequency, where lower frequencies enhance alignment ( $\zeta = 0.9$  at 100 Hz) while higher frequencies hinder it due to increased agitation as seen at 500 Hz and 1000 Hz.

The aspect ratio of the grains was also found to play a critical role in governing the order parameter. Grains with higher aspect ratio ( $AR = 4$ ) exhibit stronger alignment under lower agitation. Conversely, grains with lower aspect ratios ( $AR = 2$ ) displayed more random orientations under higher agitation. This behavior underscores the importance of grain shape in controlling alignment within the granular system.

## References

- [1] Igor S Aranson and Lev S Tsimring. “Patterns and collective behavior in granular media: Theoretical concepts”. In: *Reviews of modern physics* 78.2 (2006), pp. 641–692.
- [2] Ben Nadler. “Anisotropic inertia rheology of ellipsoidal grains”. In: *Granular Matter* 23.1 (2021), p. 14.
- [3] AA Pena, R Garcia-Rojo, and Hans Jürgen Herrmann. “Influence of particle shape on sheared dense granular media”. In: *Granular matter* 9.3 (2007), pp. 279–291.
- [4] K Anki Reddy, V Kumaran, and J Talbot. “Orientational ordering in sheared inelastic dumbbells”. In: *Physical Review E* 80.3 (2009), p. 031304.
- [5] Dániel B Nagy et al. “Rheology of dense granular flows for elongated particles”. In: *Physical Review E* 96.6 (2017), p. 062903.
- [6] Emilien Azéma, Itthichai Preechawuttipong, and Farhang Radjai. “Binary mixtures of disks and elongated particles: Texture and mechanical properties”. In: *Physical Review E* 94.4 (2016), p. 042901.
- [7] Peter A Cundall and Otto DL Strack. “A discrete numerical model for granular assemblies”. In: *geotechnique* 29.1 (1979), pp. 47–65.
- [8] Paul W Cleary. “The effect of particle shape on simple shear flows”. In: *Powder Technology* 179.3 (2008), pp. 144–163.
- [9] H Kruggel-Emden et al. “A study on the validity of the multi-sphere Discrete Element Method”. In: *Powder Technology* 188.2 (2008), pp. 153–165.
- [10] B Nadler, F Guillard, and I Einav. “Kinematic model of transient shape-induced anisotropy in dense granular flow”. In: *Physical review letters* 120.19 (2018), p. 198003.
- [11] Heinrich Hertz. “Ueber die Berührung fester elastischer Körper.” In: (1882).
- [12] *EDEM User Manual*. Altair Engineering, Inc. 2024. URL: <https://www.altair.com/edem/>.
- [13] Yutaka Tsuji, Toshitsugu Tanaka, and T Ishida. “Lagrangian numerical simulation of plug flow of cohesionless particles in a horizontal pipe”. In: *Powder technology* 71.3 (1992), pp. 239–250.
- [14] Diego Berzi and James T. Jenkins. “Fluidity, anisotropy, and velocity correlations in frictionless, collisional grain flows”. In: *Phys. Rev. Fluids* 3 (9 2018), p. 094303. DOI: 10.1103/PhysRevFluids.3.094303.